



The Society shall not be responsible for statements or opinions advanced in papers or in discussion at meetings of the Society or of its Divisions or Sections, or printed in its publications. Discussion is printed only if the paper is published in an ASME Journal. Papers are available from ASME for fifteen months after the meeting.

Printed in USA.

Copyright © 1990 by ASME

Active Stabilization of Centrifugal Compressor Surge

J. E. PINSLEY*, G. R. GUENETTE, A. H. EPSTEIN, E. M. GREITZER

Gas Turbine Laboratory
Department of Aeronautics and Astronautics
Massachusetts Institute of Technology
Cambridge, MA 02139

ABSTRACT

Active suppression of centrifugal compressor surge has been demonstrated on a centrifugal compressor equipped with a servo-actuated plenum exit throttle controller. The control scheme is fundamentally different from conventional surge control techniques in that it addresses directly the dynamic behavior of the compression system to displace the surge line to lower mass flows. The method used is to feed back perturbations in plenum pressure rise, in real time, to a fast acting control valve. The increased aerodynamic damping of incipient oscillations due to the resulting valve motion allows stable operation past the normal surge line. For the compressor used, a 25% reduction in the surge point mass flow was achieved, over a range of speeds and pressure ratios. Time-resolved measurements during controlled operation revealed that the throttle required relatively little power to suppress the surge oscillations, because the disturbances are attacked in their initial stages. Although designed for operation with small disturbances, the controller was also able to eliminate existing, large amplitude, surge oscillations. Comparison of experimental results with theoretical predictions showed that a lumped parameter model appeared adequate to represent the behavior of the compression system with the throttle controller and, perhaps more importantly, to be used in the design of more sophisticated control strategies.

NOMENCLATURE

a	speed of sound
A_{in}	impeller annulus inlet area
A_T	control valve (throttle) area
B	stability parameter defined in Eq. (A.12), $B = U/2\omega_H L_c$
$C_{throttle}$	velocity at throttle exit
C_x	axial velocity
L_c	effective compressor duct length
\dot{m}	mass flow
P_0	ambient pressure
P_p	plenum pressure
ΔP	plenum to ambient pressure difference; $\Delta P = P_p - P_0$
ΔP_c	compressor pressure rise; ambient to plenum
ΔP_T	throttle (valve) pressure drop; plenum to ambient
t	time
U	impeller exit tip speed
V_p	plenum volume

Z	complex proportionality constant for controller
ρ_0	ambient density
ϕ	non-dimensional flow coefficient; $\phi = C_x/U$
ψ	non-dimensional pressure rise; $\psi = \Delta P / 1/2 \rho U^2$
τ	non-dimensional time; $\tau = \omega_H t$
ω_H	system Helmholtz resonator frequency; $\omega_H = a\sqrt{A_{in}/V_p L_c}$
$\delta()$	perturbation quantity
(\wedge)	non-dimensional quantity
(\sim)	fluctuation
$(\bar{\quad})$	mean quantity

INTRODUCTION

Compression system surge is a self-excited instability, evidenced by large amplitude oscillations of annulus averaged mass flow and plenum pressure rise. Operation in surge often results in severely degraded performance, as well as unacceptable levels of system vibration.

To avoid surge, one commonly adopts a margin of safety between the surge line, the limit of stable operation, and the closest allowable operating point. However, this can prohibit operation in regions of highest efficiency or pressure rise. In this paper, experiments are described that demonstrate a new method for allowing operation in regimes that have been previously inaccessible, not only close to but beyond the "natural" surge line. The procedure used is the closed loop feedback control of the dynamic behavior of the compression system. As will be shown, such active control techniques, which suppress the instabilities that lead to surge, can extend the range of stable operation beyond the natural surge line and enlarge the usable compressor operating region. This, in turn, can allow greater freedom not only in compressor operation, but also in design.

Active Control of Surge

There has been much work carried out on what is termed surge control, and discussions of different available techniques have been given by Boyce (1983), Ludwig and Nenni (1980), and Staroselsky and Ladin (1979). The approach taken here is fundamentally different from these types of surge suppression schemes because it is based on affecting changes in the unsteady system response, i.e. the system dynamics, rather than the steady-state behavior. More specifically, existing surge control schemes act by effectively lowering the operating line once some steady-state, near surge operating condition is reached or detected. These strategies do not enhance stability; rather they reduce the safety margins otherwise necessary. In contrast, the

* Present Address: AVCO Research Laboratory—Textron, Everett, MA

approach described herein uses active control to enhance the stability of the compression system, effectively moving the surge line.

The conceptual basis for the active control scheme presented here is that the nonlinear limit cycle oscillations characterizing surge will start as small amplitude disturbances which then grow to a finite limit. Attacking this growth in the early stages, thus requires only low power and small amplitude control actions. The basic idea is to sense the small disturbances associated with incipient surge and feed back a signal derived from them (appropriately modified as to gain and phase) into an actuator or actuators. The combination of compressor, sensors, processors, and actuators (i.e. of compressor plus controller) constitutes a new machine, having different stability properties than the compressor alone. This can be exploited to enhance the stable flow range.

The analytical framework for this approach to active control has been developed by Epstein, Ffowcs Williams and Greitzer (1989), referred to henceforth as EFG. They used a lumped parameter representation of a compression system to examine two basic control strategies in which either (or both) an exit throttle or a collector (plenum) wall would be driven in response to sensed perturbations in the compressor discharge pressure. Calculations carried out using a simple proportional feedback control predicted that significant shifts in the surge point could be achieved. Although the compressor, the destabilizing element in the system, continues to feed energy into small amplitude perturbations, it was shown that the controller increases the capability of other parts of the system to dissipate these unsteady perturbations. In addition, the controller power requirements were shown to scale with the square of the disturbance amplitude and were thus much less than steady state machine power.

The present paper presents the experimental demonstration of these ideas for one of these schemes, that of employing a varying exit throttle area. A schematic of the system of interest with the throttle controller at the plenum exit is shown in Fig. 1. As described in EFG, this is of some interest because, for an ideal controller at least, there need be no net average power expended to drive the throttle. Controller power requirements are thus independent of compression system power, and the increased dissipation associated with the perturbations can be regarded as due to increased leverage of the existing dissipative element in the system. It is stressed that it is the dissipation in the unsteady system behavior that is modified, so that the steady-state operating point is essentially unaffected by the control.

The present work by no means attempts to define an optimum controller configuration, but is rather a proof-of-concept examination of the ideas expressed in EFG. In this connection we note two other complementary approaches to modifying the dynamic system behavior which have close links to the present study. One is by Ffowcs Williams and Huang (1989) who used a loudspeaker to drive a moving plenum wall and the other by Gysling (1989), who used a tailored structural element (a moving plenum wall with a spring and dashpot) to provide increased damping of system perturbations through coupling of the aerodynamic and structural behavior. In both of these investigations, a significant increase in stable flow range was achieved.

Scope of the Present Investigation

The aim of the experiments was to demonstrate active stability enhancement (surge suppression) using throttle control of a centrifugal compressor. To design the experiments, parametric studies were initially carried out using a lumped-parameter system model; these

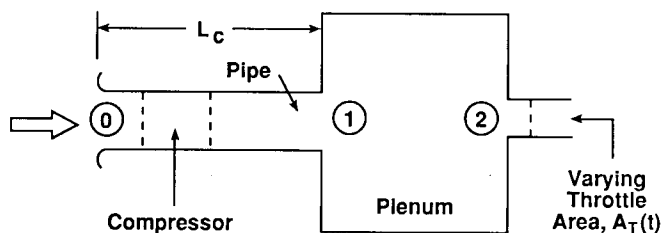


Fig. 1: Schematic of generic pumping system with active exit throttle

modelling studies also served to help interpret the experimental results. Both steady state and time resolved data were taken to characterize the system performance with and without control. The control scheme was tested over a range of system parameters, not only to assess control effectiveness over the range, but also to examine, in a diagnostic fashion, the effects of compressibility on the system dynamics.

Specifically, the investigation addressed the following questions:

- 1) Does this type of active control suppress system oscillations?
- 2) What will the system performance be in a controlled region of operation?
- 3) Will the controller adversely affect operation in normally stable regions?
- 4) Does the linear model accurately represent the system and the controller?
- 5) What parameters have the dominant influence on system controllability?
- 6) Can the results obtained in this experiment be generalized for other similar systems?

One can thus view the experiments as focused on two general goals. The first is demonstration of active control of a compression system over a range of parameters. The second is to verify that the basic modelling captures the system and controller dynamic behavior well enough so that this type of analysis can be used in future studies (and designs of) more complex control schemes.

SYSTEM MODELLING

Lumped parameter system models have been used by many authors to examine instability inception in both axial and centrifugal compression systems, e.g. Emmons, Pearson, and Grant (1955), Greitzer (1981), and Ffowcs Williams and Huang (1989), and there is no need to enter into a detailed description here. For reference, the derivation is sketched out in Appendix A, where it is shown that the non-dimensional form of the linearized equations for the behavior of the non-dimensional mass flow and pressure rise perturbations, $\delta\phi$ and $\delta\psi$, take the form:

$$\frac{d\delta\phi_1}{d\tau} = B \left(\frac{d\psi_c}{d\phi} \right) \delta\phi_1 - B \delta\psi \quad (1)$$

$$\frac{d\delta\psi}{d\tau} = \frac{\delta\phi_1}{B} - \frac{1}{B \left(\frac{\partial\psi_T}{\partial\phi} \right)_{A_T}} \delta\psi + \frac{\left(\frac{\partial\psi_T}{\partial\hat{A}_T} \right)_{\phi}}{B \left(\frac{\partial\psi_T}{\partial\phi} \right)_{A_T}} \delta\hat{A}_T \quad (2)$$

In Eqs. (1) and (2), $\delta(\cdot)$ denotes a perturbation quantity, τ is non-dimensional time, \hat{A}_T is the non-dimensional control valve area, A_T/A_{in} , and B is the system stability parameter ($B = U/2\omega_H L_c$). $d\psi_c/d\phi$ and $(\partial\psi_T/\partial\phi)_{A_T}$ are non-dimensionalized derivatives of the compressor and throttle characteristics with respect to mass flow, $(\partial\psi_T/\partial A_T)_{\phi}$ is the derivative of the valve pressure rise vs. valve area characteristic, and subscript 1 refers to compressor inlet station.

Equations (1) and (2) do not completely define the system dynamic behavior because the relation between the throttle area perturbation is not linked to the pressure rise or mass flow perturbations. Specifying this relation defines the throttle control law and, in what follows, we take the relation to be the simple proportionality, expressed in Eq. (3):

$$\frac{\delta\hat{A}_T}{\hat{A}_T} = Z \delta\psi \quad (3)$$

Z is a complex constant describing the gain and phase relations between sensed pressure perturbations and instantaneous valve area. Inserting Eq. (3) into the system equations (1) and (2) produces two coupled equations for $\delta\phi$ and $\delta\psi$. These have solutions of the form

e^{sT} where the characteristic equation for S is given by:

$$S^2 + S \left[\frac{1}{B} \left(1 - \frac{\left(\frac{\partial \psi_T}{\partial \hat{A}_T} \right)_\phi \bar{\hat{A}}_T Z}{\left(\frac{\partial \psi_T}{\partial \phi} \right)_{A_T}} \right) - B \left(\frac{d\psi_c}{d\phi} \right) \right] + \left[1 - \frac{\left(\frac{d\psi_c}{d\phi} \right)}{\left(\frac{\partial \psi_T}{\partial \phi} \right)_{A_T}} \left(1 - \frac{\left(\frac{\partial \psi_T}{\partial \hat{A}_T} \right)_\phi \bar{\hat{A}}_T Z}{\left(\frac{\partial \psi_T}{\partial \phi} \right)_{A_T}} \right) \right] = 0 \quad (4)$$

Equation (4) is the characteristic equation of a damped harmonic oscillator, with the damping either positive or negative depending on compressor operating point. In this context, the primary role of the the active control is to modify the damping term in the equation, increasing the stability of the oscillatory system.

Overall Results of System Modelling Studies

Several clear trends emerged from the parametric studies of the compression system which were performed to select the control parameters. First, as pointed out in EFG, the perturbation in area should be in phase with the plenum pressure perturbation for maximum effectiveness. (Note that this statement pertains only to the particular control strategy used here; other schemes will have different optimum phases, e.g. Ffowcs Williams and Huang (1989).) In addition, the control effectiveness decreases as either or both the B parameter and the slope of the compressor characteristic increase. Finally, for a given operating point, there is a finite range of gains and phases over which the growth of the perturbations can be suppressed. These trends imply that, for a specific operating point (specified compressor slope), the region of stability in the gain phase plane will appear as in Fig. 2, which shows typical closed regions of stable operation for four values of the B parameter.

The physical reason for the decreased effectiveness with increase in B parameter is connected to the overall decrease in stability that occurs as B increases. This is well-known, and has been amply discussed in the literature (e.g., Greitzer (1981)). Larger B implies a more compliant system, which means that the (unsteady) flow through

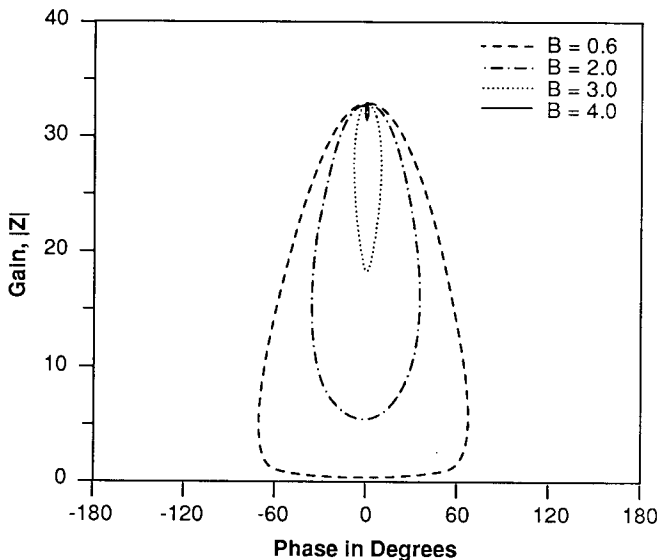


Fig. 2: Increasing B decreases variations in controller gain and phase over which the pumping system is stable (the regions within the curves); fixed operating point ($\psi=1.9$, $\phi=0.12$, $d\psi/d\phi=1.0$)

the throttle is less coupled to the unsteady flow through the compressor. Control strategies using a downstream throttle would therefore be expected to lose effectiveness. We return to this point when we discuss possible future directions for this research.

The system dynamics underlying the most effective operation occurring at zero phase have also been presented in EFG, but it is useful to summarize these arguments, since they are crucial to understanding the role of the control. The instabilities of interest occur as the result of mechanical energy being fed into the perturbations by the unsteady flow through the compressor. This energy can be offset, and the system stabilized, by dissipation in the throttle. The net (compared to the value for steady-state operation) dissipation in the throttle is proportional to the product $[\delta(\text{plenum pressure}) \cdot \delta(\text{throttle mass flow})]$. The throttle mass flow, \dot{m}_T , is

$$\dot{m}_T = \rho C_{\text{throttle}} A_T \quad (5)$$

For values of system pressure rise small compared to ambient, the velocity at the throttle exit is given by

$$C_{\text{throttle}} = \sqrt{2\Delta P_p / \rho}$$

Using this expression for C_{throttle} , and splitting quantities into time mean (denoted by $\bar{(\)}$) and perturbation (denoted by $\delta(\)$), the mass flow perturbation can be written as

$$\frac{\delta \dot{m}_T}{\bar{\dot{m}}_T} = \frac{1}{2} \frac{\delta \Delta P_p}{\Delta P} + \frac{\delta A_T}{\bar{A}_T} \quad (6)$$

For a given controller gain, the product of mass flow perturbation and pressure perturbation (i.e. the dissipation) is thus maximized when δA_T and $\delta \Delta P_p$ are in phase.

The existence of a minimum level of gain needed for system stabilization should be evident. The reason for the existence of a maximum gain can be seen by invoking the above considerations and referring to Fig. 3, which shows compressor and throttle pressure differences versus flow. Consider small perturbations in pressure about a given operating point A, as indicated. The throttle mass flow fluctuations will basically track along the throttle curve and, for a fixed throttle, the mass flow will fluctuate as shown by points b and b' on the solid curve. If the throttle area is varied to be in phase with $\delta \Delta P_p$, however, the mass flow fluctuations can be considerably increased, as

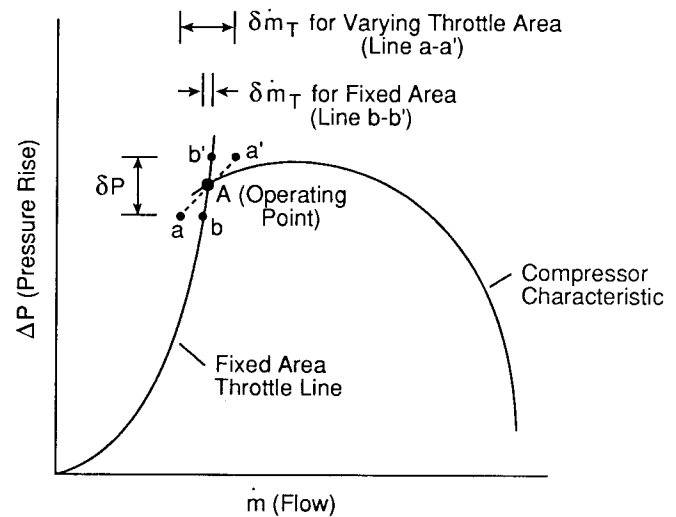


Fig. 3: Maximum system gain is reached when instantaneous throttle line (a-a') slope becomes less steep than the compressor characteristic, inducing static instability

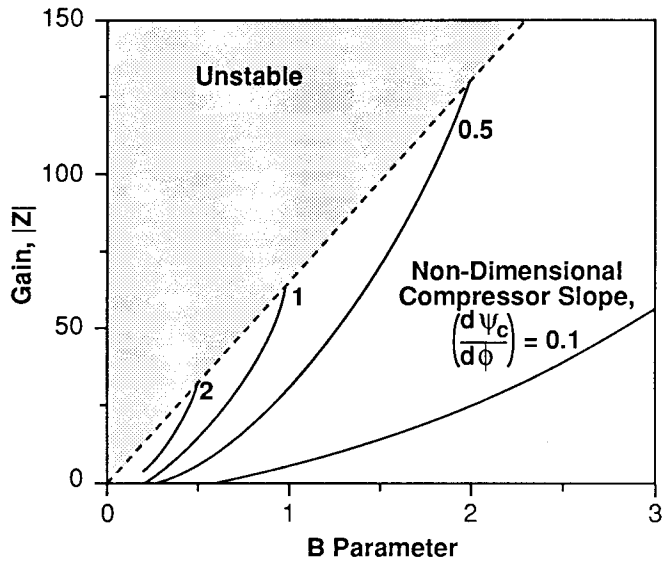


Fig. 4: Gain required to stabilize the compression system increases with increasing B and compressor slope $d\psi_c/d\phi$; $\phi = 0.12$

indicated by points a and a' on the dashed line, which represents the instantaneous throttle line seen by the system. Increasing the gain thus decreases the slope of the throttle line, relative to the fixed geometry throttle, and increases the mass flow perturbations (and hence the overall dissipation) to suppress the system dynamic instability. If the slope of the throttle line is decreased too far, however, it will become less steep than the compressor characteristic slope, so that the system becomes statically unstable. The flattest permissible slope occurs when the second bracketed term in Eq. (4) becomes equal to 0; this sets the maximum gain.

Using the above result, the requirement for the first bracketed term in Eq. (4) to be positive implies that the slope of the compressor characteristic is equal to $1/B$ at maximum gain. For given B, the limit of stabilization using the controller will thus occur at the point on the non-dimensional compressor characteristic where the slope $(d\psi_c/d\phi)$ is $1/B$. This slope can be compared with that for the natural surge point which occurs at a value of $(d\psi_c/d\phi)$ given by

$$\left(\frac{d\psi_c}{d\phi}\right) = \frac{1}{B^2 \left(\frac{\partial \psi_T}{\partial \phi}\right)_{AT}}$$

or, for a parabolic throttle curve,

$$\frac{d\psi_c}{d\phi} = \frac{\bar{\phi}}{2B^2 \bar{\psi}}$$

Figure 4 portrays these trends. The figure shows the value of gain (Z) needed to stabilize a compressor operating with a given compressor characteristic slope, as a function of B.

The analytical results indicate that surge suppression can be achieved with proportional feedback on the throttle motion. However, they are based on an idealized controller and a linearized model of the system. In a real system, there can be nonlinearity and, more importantly, unmodelled dynamics of the control system, which can limit effectiveness. Thus, one must examine experimentally the degree to which the model adequately captures the essential features of the problem.

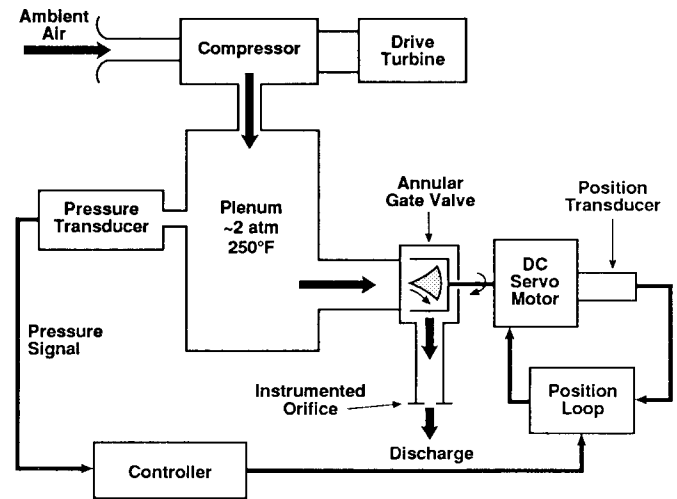


Fig. 5: Experimental setup of actively stabilized centrifugal compressor

EXPERIMENTAL FACILITY AND OVERALL TEST PARAMETERS

The turbocharger used was a Holset H1D model which has radial blades at outlet and a vaneless diffuser. Impeller tip diameter at outlet was 5.5 cm. The test stand was built to run the turbocharger at speeds near its peak efficiency region, with 110K RPM selected as the maximum compressor speed at which the controller must operate. Delivery temperature and pressure associated with this speed were roughly 150°C and 2 atm. The stand was instrumented for both transient and steady state measurements, with data acquisition through a microcomputer analog-to-digital interface. A schematic of the facility is shown in Fig. 5; more detail is given by Pinsley (1988).

The exit throttle was a rotary gate valve mounted at the plenum exit. Valve opening was set by rotating a ported inner sleeve relative to outer stationary ports. Valve angular position was measured with a rotary variable differential transformer angular displacement transducer. The pressure drop through the rotary gate valve was taken across diametrically opposed ports, so that the pressure loading on the valve was equalized around the circumference. Actuation force was applied normal to the flow and thus had only to overcome valve inertia and friction. The control valve was actuated by a low inertia DC servomotor with a rated torque of $1.07 \text{ m}^2\text{-kg/s}^2$ and a torque constant of $0.064 \text{ m}^2\text{-kg/s}^2\text{-amp}$. The inertias of the motor and valve rotors were kept as small as possible ($7.1 \times 10^{-6} \text{ kg-m}^2$ and $7.1 \times 10^{-7} \text{ kg-m}^2$ respectively) to maximize frequency response. The valve response, as tested, was flat to 80 Hz.

The compressor inlet duct length (L_c) and the plenum volume (V_p) could both be adjusted to vary the stability parameter B over a range of compressor speeds, while maintaining the system Helmholtz frequency within a relatively narrow range. This was done to minimize the possibility of encountering differing unmodeled controller dynamics at other frequencies. By changing geometries, it was possible to obtain varying B factors at a given compressor speed, or conversely the same B factor at varying compressor speeds. Table 1 summarizes the parameters corresponding to the conditions under which the controller was tested.

The area perturbation-pressure perturbation transfer function of the valve was evaluated separately by subjecting the transducer to a known pressure signal and measuring the valve response, as described by Pinsley (1988). Unless otherwise specified, all results below are with the Case I configuration.

TABLE 1
COMPRESSOR/COMPRESSION SYSTEM PARAMETERS

	Case I	Case II	Case III
V_p in m^3	0.0079	0.027	0.012
L_c in m	1.96	0.88	1.96
Compressor speed, RPMx1000	60-110	60-110	70
B parameter	.45-.72	1.26-1.93	.61
Helmholtz frequency, Hz	15.5	12.5	12.8

EXPERIMENTAL RESULTS

The effect of the controller on the compression system was evaluated from both time-averaged and time-resolved measurements. Time-resolved measurements were taken at steady state (this includes periodically varying) operating conditions, as well as during transients, in order to illustrate the unsteady system behavior.

The most basic task of the controller is to shift the surge line to lower mass flows. Time-averaged measurements of the surge line were thus made with and without the control applied. This data is also used to examine the predicted trends with variations in B parameter.

Time-resolved measurements were taken to examine the dynamics of the controlled compression system. The unsteady behavior of the compression system without the controller was first measured as baseline. The measurements were then repeated using the controller, with the compressor operating in both stable and unstable modes. Time-resolved measurements were also used to examine the predicted frequency shift due to control and the dependence of surge characteristics on the B parameter.

Time-Averaged Measurements

Compressor performance will be represented two ways: 1) in a conventional turbocharger map format: pressure ratio inlet total to plenum static vs. standard corrected flow (in ft^3/min), and 2) as a

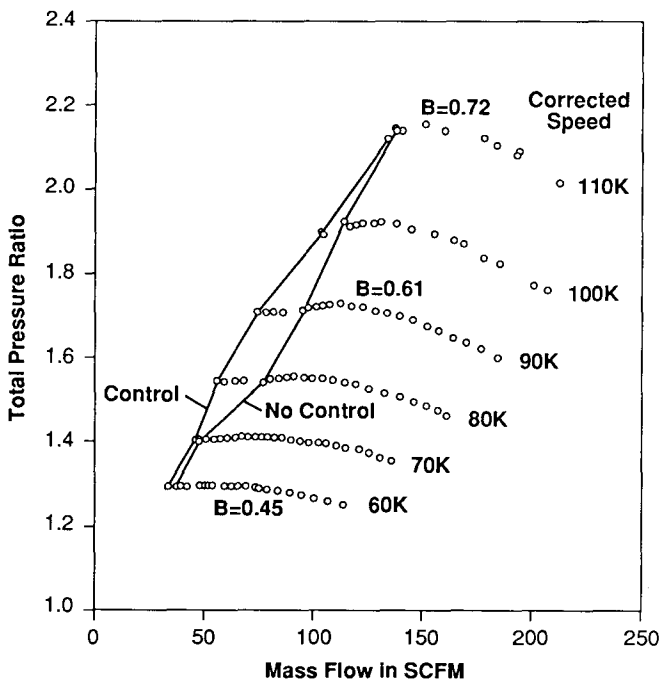


Fig. 6: Compressor map showing experimentally determined effectiveness of the active control on displacing the surge line (Case I); surge line shown as solid line

non-dimensional pressure rise

$$\psi = \frac{P_p - P_o}{\frac{1}{2} \rho_o U^2} \tag{7}$$

vs. nondimensional flow coefficient

$$\phi = \frac{C_x}{U} = \frac{\dot{m}}{\rho_o U A_{in}} \tag{8}$$

where C_x is the axial velocity at the impeller inlet annulus and U is the rotor tip speed. This is more relevant for discussion of the fluid mechanic behavior, since the compressor curves for different speeds are roughly similar.

Figure 6 shows the compressor map for Case I, in the form of pressure ratio vs. mass flow for various corrected speeds. The values of the B parameter are also indicated. Pressure ratio at surge ranges from approximately 1.3 at 60K RPM to 2.15 at 110K RPM. At the high speeds with the fixed throttle, surge occurs slightly to the left of the peak of the constant speedlines, at locations where the characteristic is slightly positively sloped. At the lowest speeds (60-70K RPM), the slope to the left of the peak is quite shallow and surge occurs at a mass flow much lower than the peak value. A "knee" in the speedline is thus observed between the 70K and 80K RPM speedlines.

Figure 6 also shows the region stabilized by the introduction of the controller. To obtain the controlled surge line, the compressor was brought close to surge on each speedline and the controller turned on at fixed gain. The control valve was closed down until the lowest attainable flow rate before deep surge (oscillations with flow reversal) was measured. The throttle was then opened, the gain increased, and the process repeated to reach another controlled operating point at the lowest stable mass flow. In these experiments the phase of the controller (i.e., the phase between pressure and throttle area perturbations) was fixed at 0 degrees since, as the theoretical results predicted, attempts made with the controller at other values of phases

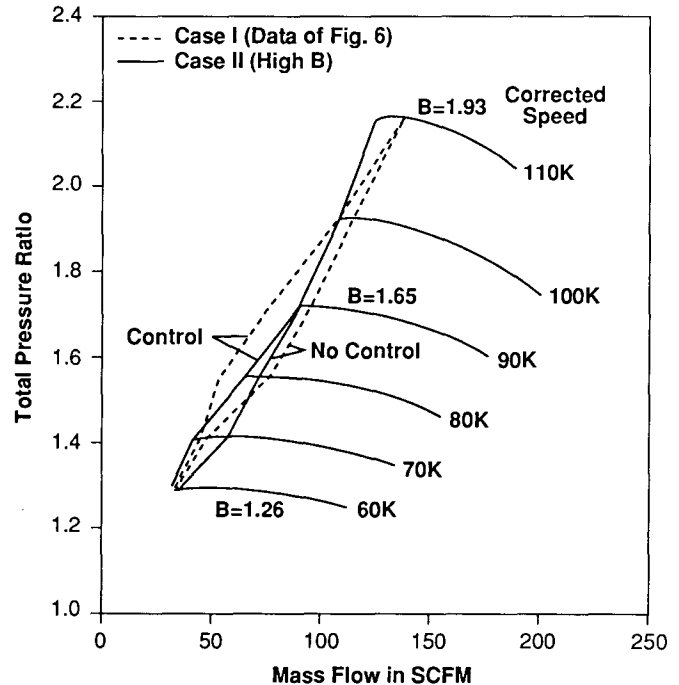


Fig. 7: Compressor map showing experimentally determined effectiveness of the active control on displacing the surge line for higher B (Case II)

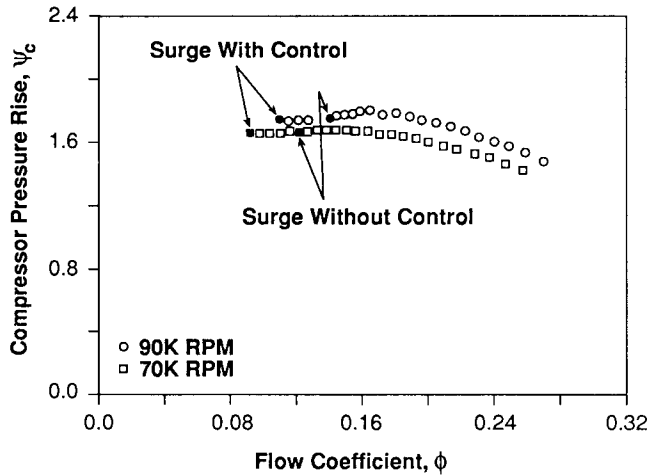


Fig. 8: 70K and 90K RPM compressor characteristics at the same value of B

were not as effective in decreasing the surge mass flow. With the control operational at 80K and 90K RPM, there was a 20-25% decrease in surge mass flow compared to the no control surge point. At 100K RPM, there was only slight extension of the stable region, while at 60-70K and 110K RPM the extension was negligible. There are thus two regimes in which the controller was ineffective: speeds below the "knee" of the surge line and high speeds. To examine the reason for this, tests were carried out at different speeds while holding B constant, as well as at different values of B holding speed constant. The tests were done to isolate effects of system dynamics from effects that had to do primarily with tip Mach number (or pressure ratio), for example, through variation of the speedline shapes. Stated another way, the goal of the parametric variations was to ensure that effects associated with tip speed alone did not limit the control scheme.

Several experiments were carried out. First, a compressor map was obtained for a system geometry with B parameter larger by a factor of 2.7 at the same compressor speed, the "Case II" configuration. The results are shown as the solid lines in Fig. 7. The knee in the surge line has shifted down in speed due to the increased B

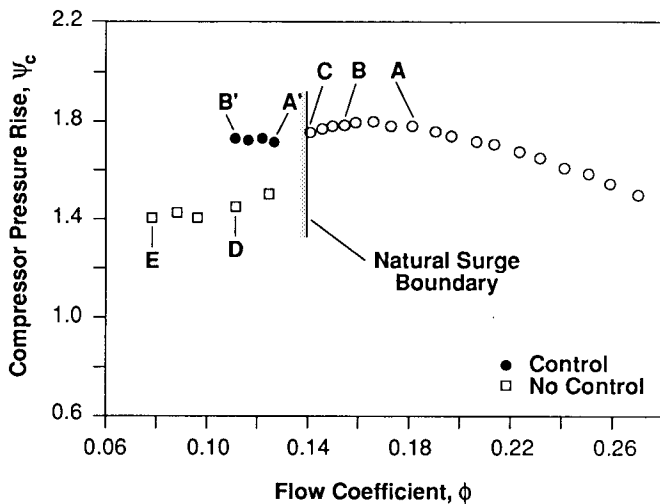


Fig. 9: Speedline indicating time-mean operating points for transient measurements

parameter with, again, no surge improvement achieved below the knee. The highest speed at which control is effective has also shifted to lower speed. Further, at speeds where control was effective, the experiments that were done at the smaller B had greater increase in stable mass flow range. As was indicated by the analysis, therefore, the B parameter plays an important role not only in determining the system stability, but also in determining the degree of control effectiveness that can be achieved.

Measurements were also made at the same value of B at two different speeds, 70K and 90K (for Case III and Case I respectively). The results are shown in Fig. 8. Although the speedlines are not quite identical and the surge point does not occur at precisely the same value of ϕ , the shifts in the surge lines due to control are similar. We infer from this that, over the range of parameters examined, it is the increase in B parameter (which represents a change in the system dynamic behavior) rather than the increase in tip Mach number which limits the effectiveness of the control.

The overall conclusions from the time-averaged measurements can be summarized as follows: the active control stabilizes the system at flows below the natural surge point; the compressor pressure rise in controlled operation remains near the pre-surge level; the control effectiveness decreases as B increases; and the position of the surge line knee is a function of B.

Time-Resolved Measurements

Although the time-averaged measurements confirmed that simple proportional control can provide significant stabilization of the system under a variety of operating conditions, the dynamic behavior of the system was also examined to explore the detailed operation of the controller. Time-resolved measurements were taken of the system

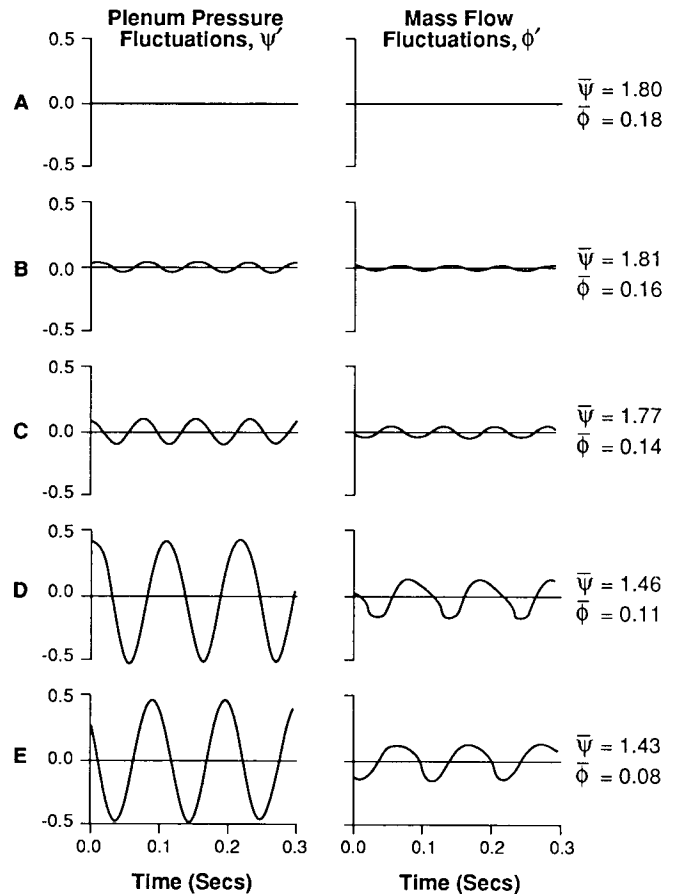


Fig. 10: Time-resolved compressor performance without control at points A-E, as indicated on Fig. 9

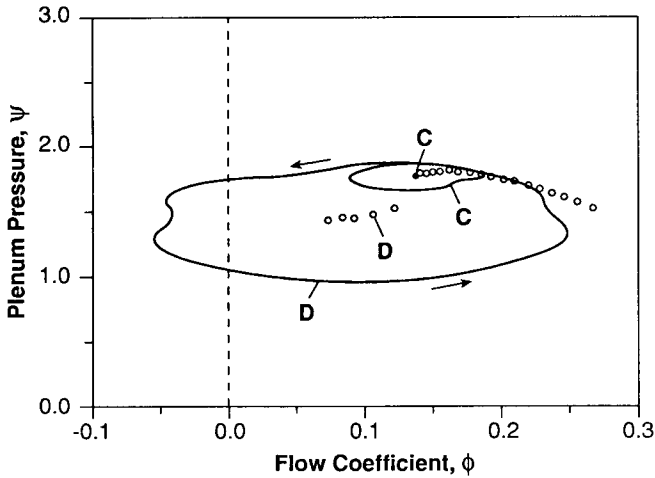


Fig. 11: Dynamic trajectory of instantaneous compressor operating points; time-mean operating points corresponding to points C and D in Fig. 9

pressure rise (inlet to plenum), and control valve area. From these, the time-resolved mass flow could be inferred from a mass flow balance, assuming an isentropic process in the plenum. The results of the measurements are presented in the time domain and in the non-dimensional pressure rise-mass flow plane. Uncertainty in the unsteady plenum pressures is less than 1% of the maximum fluctuation amplitude; uncertainty in the unsteady component of the mass flows is approximately $\pm 6\%$ for deep surge and $\pm 4\%$ for mild surge for the 90K RPM conditions shown below.

With the system in the nominal (Case I) configuration, the fluctuations in pressure rise and mass flow coefficients (ψ' and ϕ') were measured at different flow coefficients along a 90K speedline. The time-mean performance is plotted in Fig. 9 to show the conditions at which the data was taken, both with and without the control. The natural surge boundary is also indicated.

Figure 10 shows the fluctuations at points A-E, with no control applied. At point A, which lies to the right of the peak in the compressor characteristic, the compressor is operating stably. The fluctuations in pressure rise and mass flow are on the order of the noise in the system. Oscillations appear at point B, just to the left of the peak, at a frequency of 13.5 Hz, compared to the predicted Helmholtz frequency of 15.5 Hz. At this point, the slope of the compressor characteristic is very shallow and the compressor is operating in mild surge. Point C is the last stable operating point before deep surge. The compressor is still in mild surge, but the amplitude of the fluctuations has increased and the frequency has decreased slightly to 13 Hz. Points D and E show the system behavior in deep surge. The oscillations in plenum pressure and mass flow are much larger with variations in mass flow of more than $\pm 100\%$ of the steady state value. The lowering of the frequency to roughly 9 Hz is due to the time associated with plenum blowdown and repressurization (Fink, 1988).

Figure 11 portrays the dynamic behavior in the pressure-flow plane. The figure shows a mild surge oscillation, which is associated with operation at time-averaged point C, as well as a deep surge associated with operation at point D. These time-mean points are indicated for reference. The direction in which the cycles are traced out is counterclockwise. The mass flow reversal during a portion of each deep surge cycle is evident.

The points labelled A' and B' in Fig. 9 show the performance with the controller. The flow coefficient at the surge point has been shifted from 0.142 to 0.112 (at point B'), a change of 21%, and the compressor pressure rise is stabilized near the same level as prior to surge. The fluctuations in non-dimensional mass flow, pressure rise, and valve area are plotted in Fig. 12 for each indicated controlled point. The suppression of the oscillations shown in Fig. 10 is

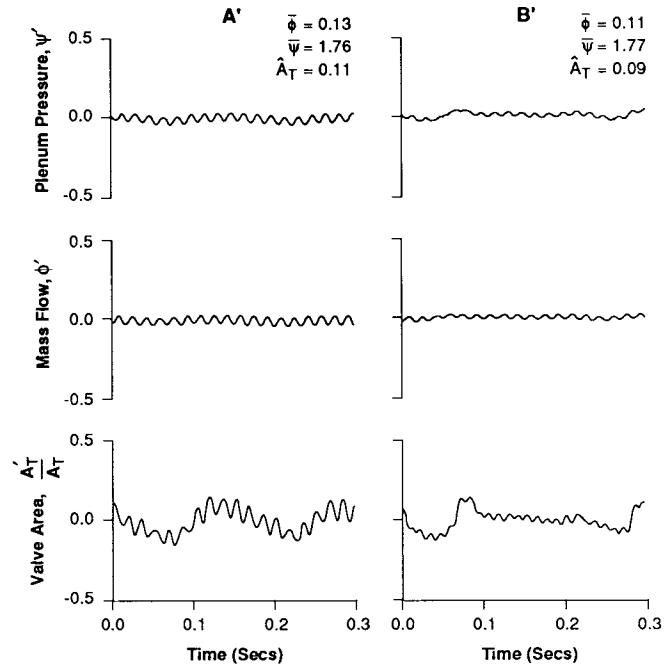


Fig. 12: Time-resolved compressor performance with controller, time-mean operating points A' and B', as indicated on Fig. 9

evident; it can also be seen that there is a higher frequency now present, with a strong component at 60 Hz. This frequency is well above any that the authors associate with system aerodynamics alone, and it is suspected that it is associated with the controller dynamics.

An alternative way to examine the effect of control on the pressure fluctuations in the system is to examine the peak amplitudes as a function of flow. This is shown in Fig. 13 for the 90K speedline. With the control, the amplitude is suppressed at flow coefficients below the natural surge value to a level below that of mild surge. Even when surge can no longer be avoided, the peak amplitude of the fluctuations remains lower than those without control.

The transient behavior of the system when the control is turned

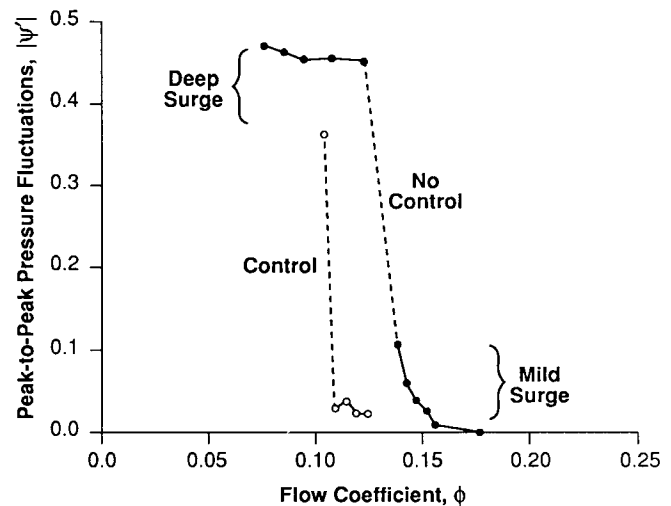


Fig. 13: Reduction in amplitude of peak pressure fluctuations with feedback control; mild surge and deep surge

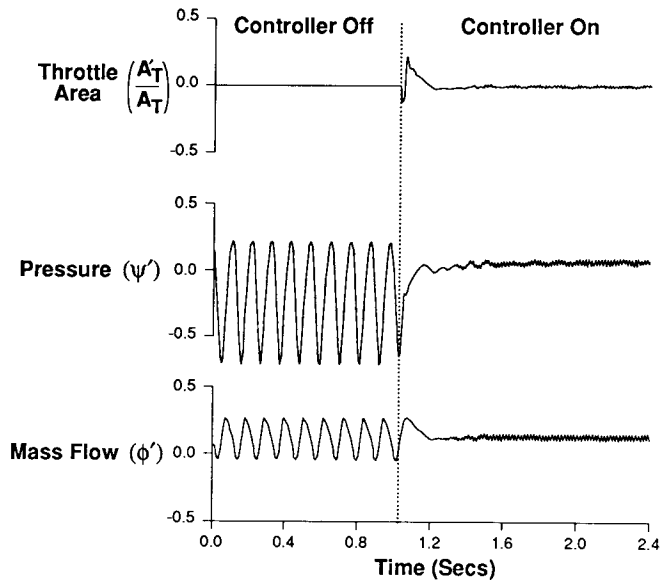


Fig. 14: Transient behavior of system initially in deep surge during controller turn-on

on or off is also of interest as a measure of control effectiveness. Figure 14 shows the non-dimensional fluctuations in the valve area and plenum pressure, as well as the variations in mass flow in the system during a transient from deep surge with the controller off, to stable operation with the controller on. (This figure can be compared with Fig. 15 in Ffowcs Williams and Huang (1989).) In the figure, time is given in dimensional form to show the actual temporal characteristics of the valve action. At $t = 1.03$ seconds, the controller is switched on at a previously set controller gain and phase. The controller captures the surge fluctuations within one to two surge cycle periods, even though the system is operating in a highly nonlinear regime. Figure 15 shows this behavior in the pressure rise-mass flow plane; the nonlinear character of the behavior prior to controller application is evident. The time mean point at the start is indicated by the solid square. Note that, although implementation of the controller shifted the time-averaged operating point along a constant throttle line from $\phi = 0.11$ to 0.12 , the stabilized operating point remains within the no-control surge region.

EVALUATION OF LUMPED PARAMETER MODEL

In this section, we examine the extent to which the simple, lumped parameter, description is useful for active control investigations. Before describing the conclusions reached with respect to model applicability, some comments are in order about the spirit in which the analysis is put forth. We have taken a very simple look at a complex dynamic system, whose parametric dependence was largely unexplored. The reasoning is that active control is a new area, and a high priority is to extract information about the central trends of the overall behavior rather than the detailed structure of the internal flow. Lumped parameter models have long been used in this regard and the comparison here is really focussed on just one aspect of their application, the use for assessing the effect of the control action. The aim is to verify this for the present system, so as to have a reliable tool for exploring more sophisticated schemes.

In applying a lumped (or even distributed) parameter analysis, one must develop a model for the energy addition due to the compressor, which is the active element in the system. In keeping with the above intent, we have taken the compressor performance as quasi-steady so that the steady-state measured characteristic is used to represent the dynamic behavior. The steady-state characteristic can be obtained down to flows beyond the surge points shown in Figs. 6 and 7 by running the compressor with a close-coupled throttle valve. This

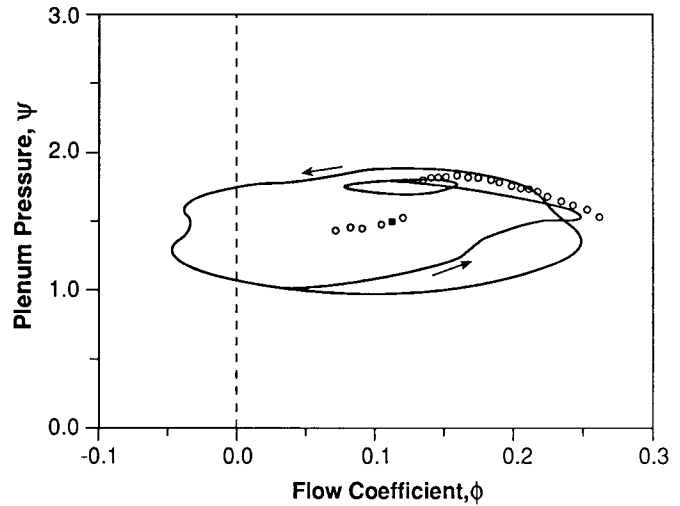


Fig. 15: Dynamic trajectory of instantaneous compressor operating point during controller turn-on transient; system initially in deep surge

greatly decreases the system volume (and hence the B-parameter) and increases the system stability (Dussord et al., 1977). In the present series of experiments, the throttle valve was placed at exit of a short pipe downstream of compressor discharge, so that the volume was reduced by a factor of twenty (B-parameter reduction of roughly 4.5). The results of doing this are shown in Fig. 16, which is a compressor map for the close coupled configuration. The instability onset points for the close-coupled geometry are shown as solid shades. Also indicated on the figure, by the dashed line, is the surge line for the previous, Case I, configuration (Fig. 6). The large difference in stable flow range will be discussed subsequently; here we merely note

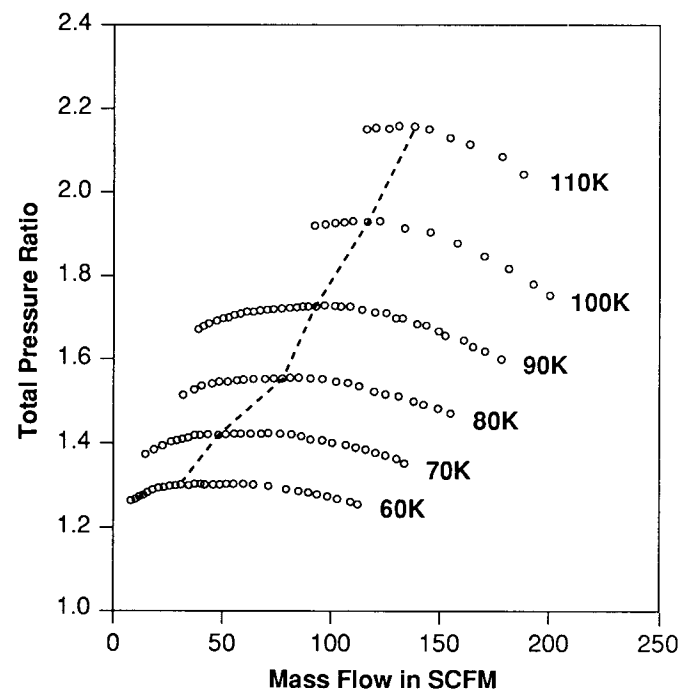


Fig. 16: Compressor map with close-coupled throttle to increase stable flow range

that the compressor characteristic is defined over a sufficient range that there need be no extrapolation for any of the stability computations that are discussed.

The most global considerations are those of system stability. Figure 17 thus shows the experimentally measured surge inception (solid line) for Case I, both with and without control, superimposed on compressor characteristics which are a ninth order fit to the actual data. Two sets of theoretical calculations of the instability onset are also shown: one based on the ninth order fit that is shown, and one based on a third order fit. We show both because we have examined the effects of various other fitting schemes, and these are a good representation of the spectrum of those used.

Two points that can be made concerning the results are shown. One is that the trends of the theory and data are in agreement at the speedlines where the control is effective, although precise quantitative predictions of the surge point are not achieved. The diminishment of control effectiveness at high and low speeds, however, is not well predicted. The second point is that, for the types of fits we examined, small changes in the fitting procedure (and thus the local slope of the curve) significantly change the predicted instability point. Thus, one can capture the trends in stability quite well with lumped parameter models, but uncertainties in the local slopes make precise prediction of absolute values difficult. Further comments on the ability of the basic model to illustrate system transients are given by Gysling (1989) and Fink (1988). They also conclude that the lumped parameter model is extremely useful for understanding the system behavior, but that precise numerical values for mass flow at instability onset are too much to ask for these flat compressor characteristics.

Beyond the stability prediction, one can examine other aspects of the system behavior. One prediction, discussed previously, is that there is a closed region in the controller gain-phase plane where stable operation may be achieved. The stable gain range decreases as the phase is shifted either positively or negatively from zero, so that at a large enough magnitude of controller phase, no amount of gain will stabilize the system. Comparison between the measured stability boundary and the theoretical prediction is made at 90K speed for the nominal configuration (Fig. 18). In carrying out the calculations, the compressor characteristic slope was set to match the maximum gain at

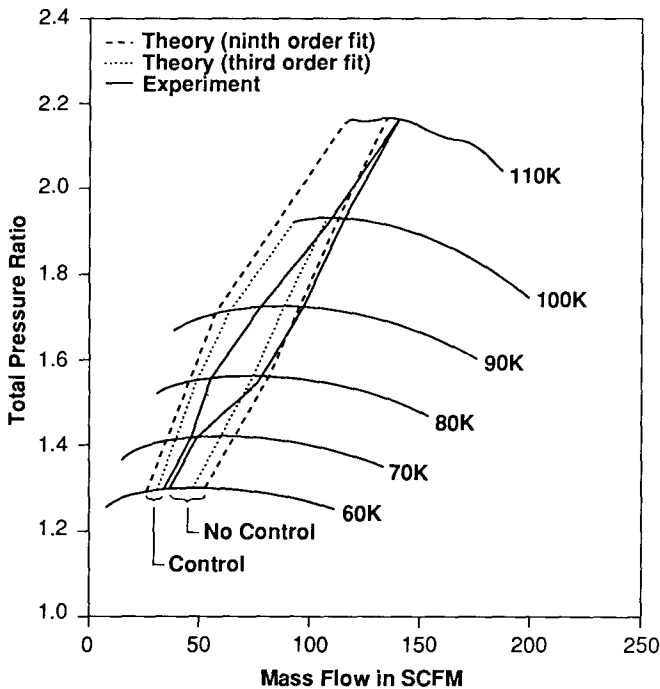


Fig. 17: Comparison of measured and theoretical compressor stability boundaries, with and without control

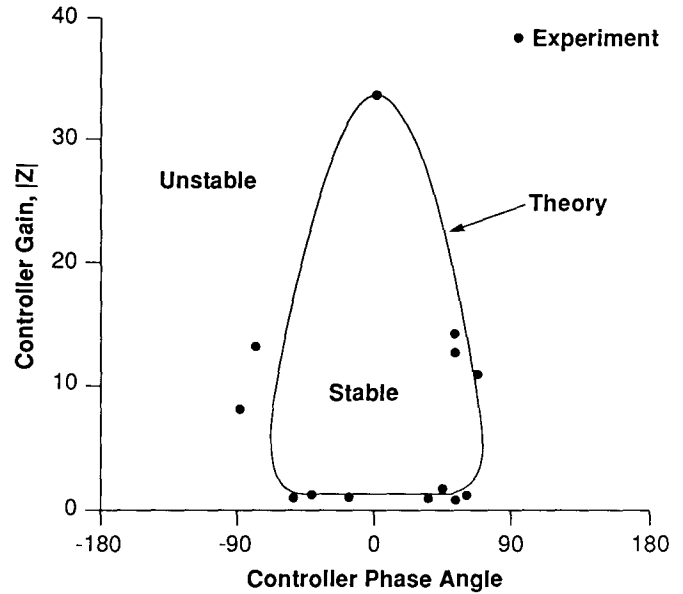


Fig. 18: Comparison of experimental and theoretical stability boundary in gain-phase space

zero degrees phase and the steady-state values of ϕ and ψ were taken from measurements.

A further test of the modelling is implied by Eq. (3), which shows that application of the control will change the frequency of small amplitude oscillations in the system. In particular for Z real and positive the frequency will decrease, and for Z real and negative the frequency will increase. As shown by Ffowcs Williams and Huang (1989), examination of this frequency shift also provides a useful diagnostic of the applicability of the modelling. In practice, with the present configuration, the frequency shift could only be measured while the system was in deep surge with the controller on, so that comparison is really being made between the linearized model and the strongly nonlinear oscillations encountered subsequent to the onset of instability. The results are shown in Fig. 19 for theoretical and measured frequency shifts. The frequency shift at 0° phase shift is roughly 20% and, with phase near 270° , the frequency is driven higher than in natural surge.

DISCUSSION AND COMMENTS ON FUTURE RESEARCH

The experiments reported on here basically represent a proof of concept demonstration that active control can be an effective means of suppression of centrifugal compressor surge. The present strategy is by no means optimal and, in fact, one reason for choosing it was that the different system components were felt to be (relatively!) easily understood and integrated. Studies have been carried out since the throttle control experiments were completed, and these indicate that one can avoid the strong fall-off in effectiveness with B by using alternative methods (Simon, 1989). In particular, one approach that has been explored analytically is to position the valve downstream of the compressor, between compressor and plenum.

As mentioned, the stabilizing effect of a close coupled throttle has been demonstrated previously (Dussourd, 1976) using a steady state device. The effect in the present system was illustrated in Fig. 16, which showed substantial range increase with reference to the nominal Case I surge line. To obtain this range, however, it was necessary to take a large pressure drop across the close coupled throttle, and this can be unacceptable in practice. This is not true, however, if one uses a time-varying throttle. While there is a trade between the time-averaged pressure drop that one takes across a close-coupled throttle and the increase in stable flow range, the pressure drops appear, from

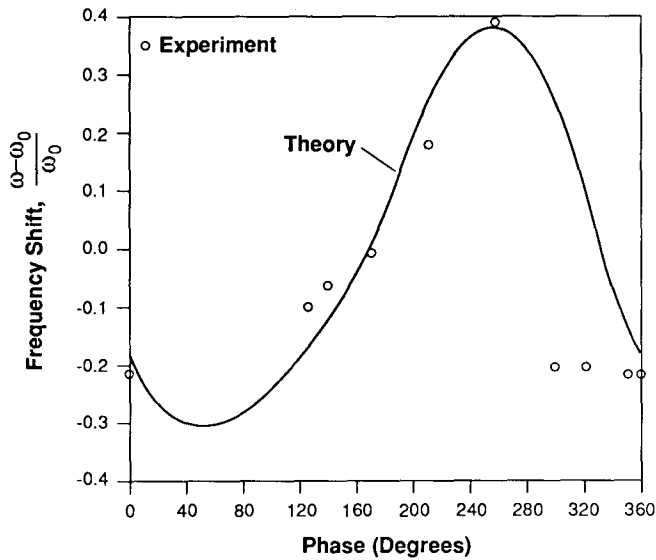


Fig. 19: Shift of system oscillatory frequency with controller phase

calculations we have carried out so far (Simon, 1989), to be considerably less than with fixed area devices. Implementation of such close coupled controls in compression systems appears to offer considerable potential and is a topic that is being aggressively pursued.

SUMMARY AND CONCLUSIONS

A theoretical and experimental study has been carried out on active control of centrifugal compressor surge. The experiments, which utilized a fast-acting downstream throttle valve, demonstrate that it is possible to suppress the growth of small amplitude perturbations, thereby stabilizing the system, and allowing operation in previously inaccessible, because unstable, regimes. Specifically, with the controller, the minimum mass flow for stable operation was reduced by 20-25% from the natural surge point, with no degradation in system performance. Further, even in surge, the controlled system exhibited smaller pressure oscillations than the system without control. Because the control strategy is based on suppression of small disturbances before they grow into surge, the power needed and the amount of activation can be extremely small.

Lumped parameter models appear to be adequate to capture the primary characteristics of the system behavior. Such models predict that effectiveness of control is strongly dependent on the system B parameter and the slope of the compressor characteristic; these trends were confirmed experimentally.

The control achieved with the very simple proportional control scheme used suggests that significant improvements are likely with more complex controllers or with different mechanisms/locations for the actuation. Active control thus appears as a promising tool for increasing the range of stable operation and thus relaxing constraints on compressor operation.

ACKNOWLEDGEMENTS

Support for this work was provided by the Army Aeropropulsion Laboratories, Mr. L. Schuman program monitor. This support is gratefully acknowledged. The help of Dr. H.G. Weber of the Cummins Engine Company in sorting out subtleties of turbocharger operation is much appreciated, as is the aid of Mr. J.O. Paduano in bringing the motor controller from concept to reality. Initial valve design and preliminary low speed experiments were carried out by Mr. G. Haldeman. We are most grateful to Mr. J. Simon for useful discussions about the system dynamics, for resolving some

discrepancies in the data analysis procedure, and for carrying out calculations shown in Fig. 17. We also wish to acknowledge that J.E. Pinsley was supported by a traineeship under the AFOSR Air Force Research in Aero Propulsion Technology (AFRAPT) Program.

REFERENCES

- Boyce, M.P. et al., 1983, "Tutorial Session on Practical Approach to Surge and Surge Control Systems," in *Proceedings of the Twelfth Turbomachinery Symposium*, Texas A&M University Turbomachinery Laboratories.
- Dussourd, J.L., Pfannebecker, C.W., and Singhania, S.K., 1977, "An Experimental Investigation of the Control of Surge in Radial Compressors Using Close Coupled Resistances," *ASME J. Fluids Eng.*, Vol. 99, pp. 64-76.
- Epstein, A.H., Ffowcs Williams, J.E., and Greitzer, E.M., 1989, "Active Suppression of Aerodynamic Instabilities in Turbomachines," *J. Propulsion and Power*, Vol. 5, March-April pp. 204-211.
- Ffowcs Williams, J.E., and Huang, X., 1989, "Active Stabilization of Compressor Surge," *J. Fluid Mechanics*, Vol. 204, pp. 245-262.
- Fink, D.A., 1988, "Surge Dynamics and Unsteady Flow Phenomena in Centrifugal Compressors," MIT Gas Turbine Laboratory Report No. 193.
- Greitzer, E.M., 1981, "The Stability of Pumping Systems -- The 1980 Freeman Scholar Lecture," *Journal of Fluids Engineering*, Vol. 103, pp. 193-242.
- Gysling, D.L., 1989, "Dynamic Control of Centrifugal Compressor Surge Using Tailored Structure", M.S. Thesis, Department of Aeronautics and Astronautics, Massachusetts Institute of Technology.
- Ludwig, G.R., and Nenni, J.P., 1980, "Tests of an Improved Rotating Stall Control System on a J-85 Turbojet Engine," ASME Paper 80-GT-17.
- Pinsley, J.E., 1988, "Active Control of Centrifugal Compressor Surge," M.S. Thesis, Department of Aeronautics and Astronautics, Massachusetts Institute of Technology.
- Simon, J., 1989, Private Communication.
- Staroselsky, N., and Ladin, L., 1979, "Improved Surge Control for Centrifugal Compressors," *Chemical Engineering*, pp. 175-184.

APPENDIX: DERIVATION OF THE SYSTEM EQUATIONS

Consider the compression system shown in Fig. 1. The following assumptions are made: quasi-steady compressor and throttle behavior; uniform pressure throughout the plenum; isentropic behavior in the plenum; incompressible one-dimensional flow in the ducts; and negligible throttle inertia.

The integral form of the one-dimensional momentum equation for the compressor duct is

$$P_0 - P_1 = \rho \frac{dC_x}{dt} L_c - \Delta P_c \quad (A.1)$$

where L_c is an equivalent compressor duct length chosen to give the same dynamic response as the actual system. In terms of compressor mass flow, this can be written as:

$$P_0 - P_1 = \frac{L_c}{A_{in}} \frac{dm_1}{dt} - \Delta P_c \quad (A.2)$$

The equation for the throttle duct pressure drop is:

$$P_1 - P_0 = \Delta P_T \quad (A.3)$$

where ΔP_T is the pressure drop across the throttle.

The throttle and compressor mass flows are linked by mass conservation in the plenum:

$$\dot{m}_1 = \dot{m}_2 + V_p \frac{d\rho_p}{dt} \quad (\text{A.4})$$

where V_p is the plenum volume. Using the isentropic relation, this becomes

$$\dot{m}_1 = \dot{m}_2 + \frac{V_p}{a_1^2} \frac{dP_p}{dt} \quad (\text{A.5})$$

Equations (A.2), (A.3), and (A.5) describe the unsteady behavior of the compression system. To examine the system stability, the equations are linearized about a mean operating point, with flow variables written as:

$$(\cdot) = \overline{(\cdot)} + \delta(\cdot) \quad (\text{A.6})$$

The compressor pressure rise is

$$\Delta P_c = \overline{\Delta P_c} + \left. \frac{d\overline{\Delta P_c}}{d\dot{m}_1} \right|_{\dot{m}_1} \delta \dot{m}_1 \quad (\text{A.7})$$

Equation (A.7) is based on the assumption that the instantaneous compressor pressure rise/flow characteristic is quasi-steady. It is shown by Fink (1988) and Gysling (1989) that this is not precisely true but that the effect on stability, which is the point investigated here, is small.

The throttle pressure drop is given by

$$\Delta P_T = \overline{\Delta P_T} + \left. \left(\frac{\partial \overline{\Delta P_T}}{\partial \dot{m}} \right)_{A_T} \right|_{\dot{m}} \delta \dot{m}_2 + \left. \left(\frac{\partial \overline{\Delta P_T}}{\partial A_T} \right)_{\dot{m}} \right|_{\dot{m}} \delta A_T \quad (\text{A.8})$$

In Eqs. (A.7) and (A.8), overbars designate mean flow properties and A_T is the throttle valve area.

We non-dimensionalize the pressures by $1/2 \rho_0 U^2$, the flow by $\rho_0 U A_{in}$, the time by $1/\omega_H$ (where ω_H is the Helmholtz resonator frequency of the system, defined in the nomenclature), and the areas by A_{in} . The non-dimensional pressure and flow are denoted by ψ and ϕ . In addition, we define the non-dimensional stability parameter, B , as:

$$B = \frac{U}{2\omega L_c} = \frac{U}{2a_1} \sqrt{\frac{V_p}{L_c A_{in}}} \quad (\text{A.9})$$

We utilize the non-dimensional derivatives of the compressor and throttle in the expression for compressor pressure rise and throttle pressure drop perturbations as follows:

$$\delta \psi_c = \left(\frac{d\overline{\psi_c}}{d\phi} \right) \delta \phi_1 \quad (\text{non-dimensional compressor pressure rise})$$

$$\delta \psi_T = \left(\frac{\partial \overline{\psi_T}}{\partial \phi} \right)_{A_T} \delta \phi_2 + \left(\frac{\partial \overline{\psi_T}}{\partial \widehat{A}_T} \right) \delta \widehat{A}_T$$

where \widehat{A}_T is the non-dimensional area A_T/A_{in} .

Using Eqs. (A.7) and (A.8) in Eqs. (A.2), (A.3), and (A.5), and non-dimensionalizing, the resulting three equations can be combined into two, first order, linearized equations involving $\delta \phi$, the non-dimensional compressor mass flow perturbation, and $\delta \psi$, the non-dimensional plenum pressure perturbation. These are Eqs. (1) and (2) in the main text.